

Mechanical and thermophysical properties of carbon/carbon composites with hafnium carbide

Cuiyan Li, Kezhi Li*, Hejun Li, Haibo Ouyang, Yulei Zhang, Lingjun Guo

The State Key Laboratory of Solidification Processing, Northwestern Polytechnical University, 127# Youyi Road, Xi'an 710072, Shaanxi, PR China

Received 18 December 2012; received in revised form 3 January 2013; accepted 3 February 2013

Available online 11 February 2013

Abstract

Carbon/carbon (C/C) composites with addition of hafnium carbide (HfC) were prepared by immersing the carbon felt in a hafnium oxychloride aqueous solution, followed by densification and graphitization. Mechanical properties, coefficients of thermal expansion (CTE), and thermal conductivity of the composites were investigated. Results show that mechanical properties of the composites decrease dramatically when the HfC content is greater than 6.5 wt%. CTE of the composites increases with the increase of HfC contents. The composites with addition of 6.5 wt% HfC show the highest thermal conductivity. The high thermal conductivity results from the thermal motion of CO in the gaps and pores, which can improve phonon–defect interaction of the C/C composites. Thermal conductivities of the composites decrease when the HfC content is greater than 6.5 wt%, which is due to formation of a large number of cracks in the composites. Cracks increase the phonon scattering and hence restrain heat transport, which results in the decrease of thermal conductivity of the composites.

© 2013 Elsevier Ltd and Techna Group S.r.l. All rights reserved.

Keywords: B. C/C composites; C. Mechanical properties; D. Carbides; Thermophysical properties

1. Introduction

Carbon/carbon (C/C) composites are one of the most promising high temperature structure materials due to their excellent high temperature strength, high thermal conductivity, low coefficient of thermal expansion (CTE), and good ablation resistance [1,2]. However, the poor oxidation resistance of carbon limits its high temperature applications. To improve the ablation resistance of C/C composites in the severe ablative environment, introducing refractory metal carbides into the composites has been employed. Researches on the C/C composites with addition of refractory carbide (such as zirconium carbide, tantalum carbide, and hafnium carbide) have been reported [3–6], which focus on the effect of carbides content, distribution and particle dimension on the ablation resistance of the C/C composites.

Ablation is an erosive phenomenon with removal of material by a combination of thermomechanical,

thermochemical, and thermophysical mechanisms in a severe high temperature environment [7]. Recently, researches focus on thermophysical properties of ultra-high temperature ceramics (such as ZrC, HfC, ZrB₂–ZrC–SiC, and ZrB₂–ZrC–SiC–Si₃N₄) and refractory metal with addition of carbide (such as ZrC–Mo, and ZrC–W) in the ablation application [8–12]. It is found that thermophysical properties play an important role in the oxidation and ablation of ultra-high temperature ceramics. The materials with low CTE and high thermal conductivity tend to have impressive thermal shock resistance, as the thermal gradients are minimized by increasing heat conduction of heated zone and increasing the thermal stresses in the materials. However, few researches focus on thermophysical properties of the C/C composites with addition of carbides.

In this paper, the C/C composites with addition of HfC were prepared by immersing the carbon felt in a hafnium compound aqueous solution, followed by densification and graphitization. Thermophysical and mechanical properties of the composites were studied. The heat conduction mechanism of the composites was investigated.

*Corresponding author. Tel./fax: +86 29 88495764.

E-mail address: likezhi@nwpu.edu.cn (K. Li).

2. Experimental

2.1. Preparation of the composites

Integral needle punching carbon fiber felts with a density of 0.20 g/cm^3 were used as the preforms for fabrication of the composites. The felts were formed by alternatively stacking the carbon fabric, short cut fiber web as $0^\circ/90^\circ/0^\circ/90^\circ$ (X – Y direction) pierced with carbon fiber bundles in the Z direction. Hafnium oxychloride octahydrate ($\text{HfOCl}_2 \cdot 8\text{H}_2\text{O}$, analytical grade, made by Sinopharm Chemical Reagent Co., Ltd., Shanghai, China) was used as HfC precursor.

The C/C composites with addition of HfC were prepared by the following process. Firstly, carbon fiber felts were impregnated in a hafnium oxychloride (HfOCl_2) aqueous solution with the assistance of ultrasonic. The content of HfC was controlled by the impregnation time and cycles. The impregnated felts were dried at 150°C and treated at 600°C in a nitrogen atmosphere to convert the HfOCl_2 into HfO_2 . Secondly, the carbon fiber preform was put into a thermal gradient chemical vapor infiltration (TCVI) furnace. Pyrolytic carbon was deposited in the carbon fiber preform. Methane was used as carbon source in densification. Finally, the composites were graphitized at 2500°C for 2 h in an argon atmosphere. Pure C/C composites were prepared with the same TCVI and graphitization history.

2.2. Tests and characterization

The calculation of mass content of HfC in the C/C composites was based on

$$C_{\text{HfC}} = \frac{M_{\text{HfC}}(m_1 - m_0)}{M_{\text{HfO}_2}} / m \quad (1)$$

where C_{HfC} is the mass content of HfC in the composites, m_0 is the mass of carbon felt before impregnation, m_1 is the mass of carbon felt after impregnation and heat treatment, m is the final mass of the composites after graphitization, $(m_1 - m_0)$ refers to the mass of HfO_2 remaining in the carbon fiber felt. M_{HfC} is the molecular weight of HfC, and M_{HfO_2} is the molecular weight of HfO_2 .

Compressive tests were performed on a universal testing machine using cylindrical specimen ($\Phi 6 \text{ mm} \times 9 \text{ mm}$). The tests were carried out with a constant speed of 0.2 mm/min at room temperature. Three-point bending test was carried out on the electron universal testing machine (CSS-1110). Specimens dimension was $55 \times 10 \times 4 \text{ mm}^3$. The support span was 40 mm and the span-to-thickness ratio was 10:1. Specimens were tested with a speed of 0.5 mm/min . Flexural strength and flexural modulus was calculated by the following equations:

$$\sigma_f = \frac{3PL}{2bh^2} \quad (2)$$

$$E_f = \frac{\Delta PL^3}{4bh^3 \Delta f} \quad (3)$$

where L is the span of bend test, h is the thickness, and b is the width of specimen. $\Delta P/\Delta f$ is the slope of the straight line of the load–displacement curve.

CTE of the composites was measured by a thermomechanical analyzer (DIL402C) ranging from 30 to 1300°C . The sample dimension was $3.5 \times 3.5 \times 20 \text{ mm}^3$. Thermal diffusivity and specific heat capacity of the composites were measured by a TC-3000 thermal properties analyzer. The sample dimension was $\Phi 10 \times 2.5 \text{ mm}^2$. Thermal conductivity of the composites was calculated by

$$\lambda = \alpha C_p \rho \quad (4)$$

where α is thermal diffusivity, C_p is specific heat capacity at constant pressure, and ρ is density of the composite.

A polarized light microscope (PLM, Leica DMLP) was used for the characterization of microstructure of the composites. The phase composition and morphology of the composites were investigated by X-ray diffraction (XRD, Cu-K α , X'Pert HighScore) and scanning electron microscopy (SEM, JSM6460).

3. Results and discussion

3.1. Phase analysis

Fig. 1 shows XRD patterns of the composites. The composites are composed of carbon and HfC. It is indicated that the impregnated HfO_2 is converted into HfC after graphitization. With the increase of HfC content, the

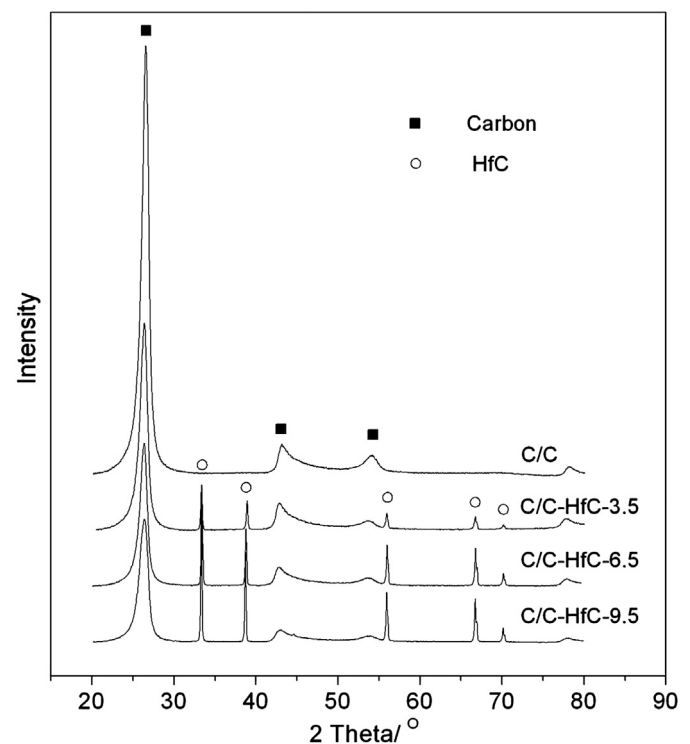


Fig. 1. XRD patterns of the C/C composites with addition of HfC.

Table 1
XRD results of the C/C composites with different added contents of HfC at the (002) plane of carbon.

Samples	d_{002} (nm)	Graphitization rate (%)
C/C	0.3357	96.5
C/C–HfC-3.5	0.3373	77.9
C/C–HfC-6.5	0.3399	47.6
C/C–HfC-9.5	0.3415	29.1

intensity of HfC peak increases and that of the carbon peak decreases. XRD results of the carbon (002) plane are listed in Table 1. The interplanar spacing of carbon (002) plane increases and graphitization rate decreases with the increase of HfC content. The XRD results suggest that adding HfC into the C/C composites restrict graphitization of the carbon.

3.2. Microstructure

Fig. 2 shows PLM micrographs of the C/C composites with and without addition of HfC. As shown in Fig. 2(a), the carbon matrix presents high optical activity in the pure C/C composites, which indicates a smooth laminar microstructure. As for the C/C composites with addition of HfC (Fig. 2(b)), the dark region is HfC and the gray region is pyrolytic carbon. HfC prefers to aggregate around the carbon fiber, especially in the fiber bundles. The pyrolytic carbon around the HfC particles is optically isotropic, which indicates an isotropic microstructure.

Fig. 3 shows SEM morphology of the composites. The growth of pyrolytic carbon in the pure C/C composites presents the layer growth characteristics (Fig. 3(a)). Adding HfC into the composites affects the growth of pyrolytic carbon. The pyrolytic carbon in the composites with addition of HfC presents the particle growth characteristics (Fig. 3(b)). Associated with the XRD results, it can be inferred that introducing HfC into the C/C composites restricts graphitization of the deposited pyrolytic carbon.

3.3. Mechanical properties

Mechanical properties of the composites are listed in Table 2. Compressive strength of the composites increases with the increase of HfC contents when HfC content is less than 6.5 wt%, and decreases when HfC content is greater than 6.5 wt%. The flexural strength of composites decrease drastically when the HfC content is greater than 6.5 wt%. Compressive properties of the composites are improved by addition of HfC, due to its high hardness and strength. The decrease of mechanical properties is resulted from the increase of cracks in the composites, as it is sensitive to cracks. Fig. 4 shows cracks in the C/C composites with addition of HfC. It can be found that the cracks are mainly distributed in the HfC aggregation region. The cracks are generated in the composites due to the mismatch of CTE between HfC and carbon matrix. Formation of cracks

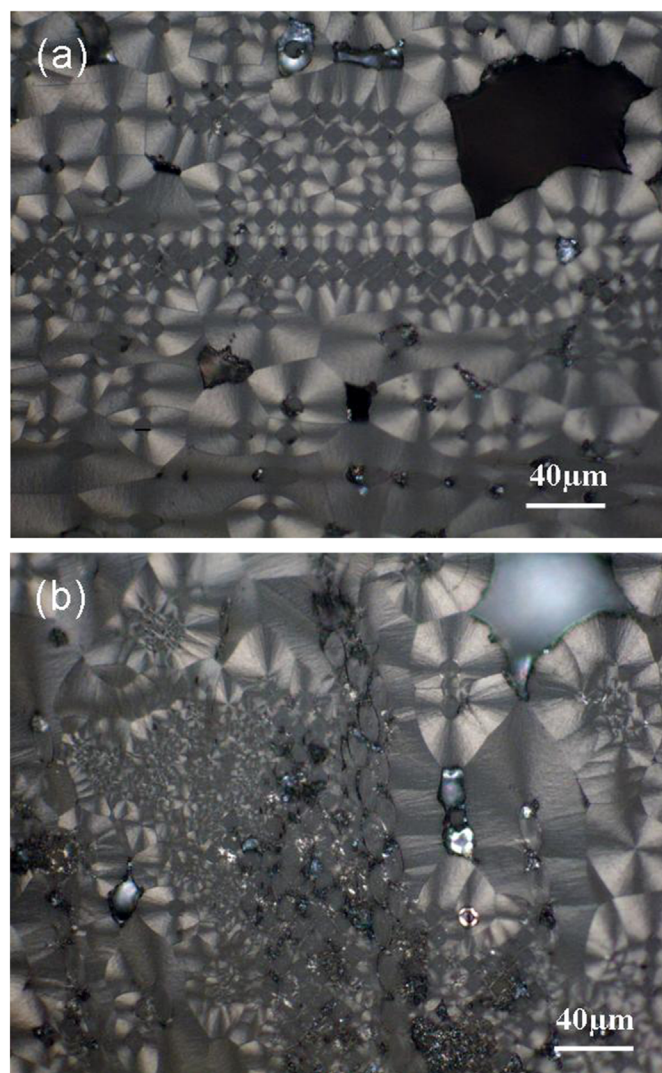


Fig. 2. Polarized light optical micrographs of the composites (a) pure C/C composites and (b) C/C composites with addition of 9.5 wt% HfC.

increases with the increase of HfC content, which causes the decrease of the mechanical properties of composites.

Fig. 5 shows the load–displacement curves of the C/C composites with addition of HfC during flexural tests. It can be seen that the pure C/C composites present the obvious pseudoplastic fracture characteristics. The elastic deformation at first occurs on the sample under flexural load, and the curve at this stage shows a linear relationship between displacement and load. Meanwhile, the flexural

load reaches its maximum and then decreases gradually for the pure C/C composites. With the increase of HfC content, the displacement of sample decreases and the slope of the straight line of load–displacement curve increases. It is indicated that the flexural modulus increases with the increase of HfC content. Moreover, the pseudo-plastic characteristics of the composites disappear gradually. The composite with 9.5 wt% HfC added presents brittle fracture.

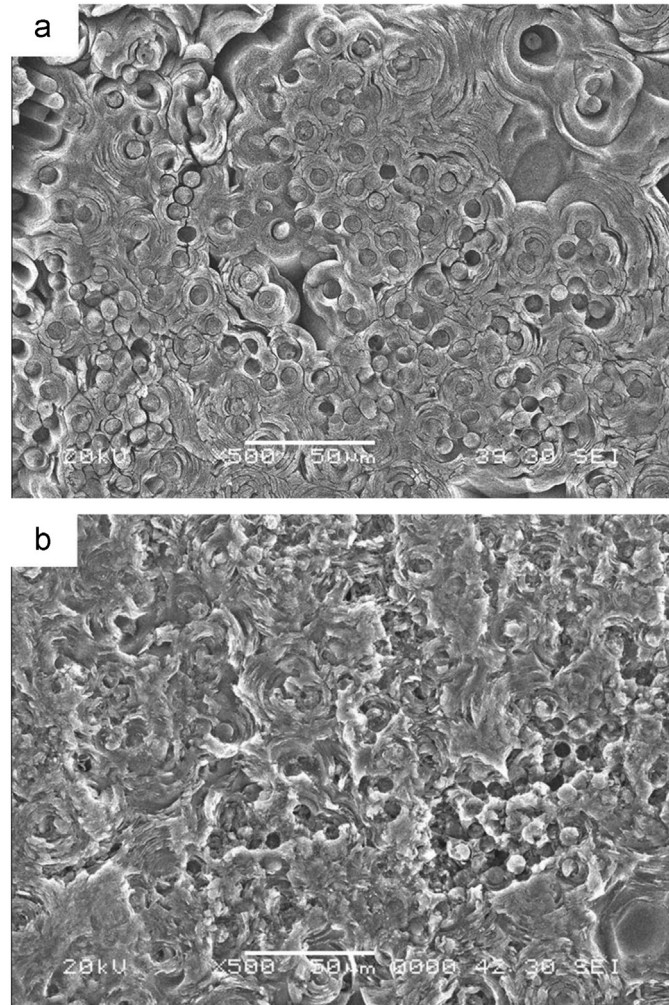


Fig. 3. SEM micrographs of the composites: (a) pure C/C composites and (b) C/C composites with addition of 9.5 wt% HfC.

The fracture morphology of pure C/C and C/C composites with addition of HfC is shown in Fig. 6. Obviously, fiber pull-out can be seen in the fracture surface of pure C/C composites (Fig. 6(a)). The C/C composites with

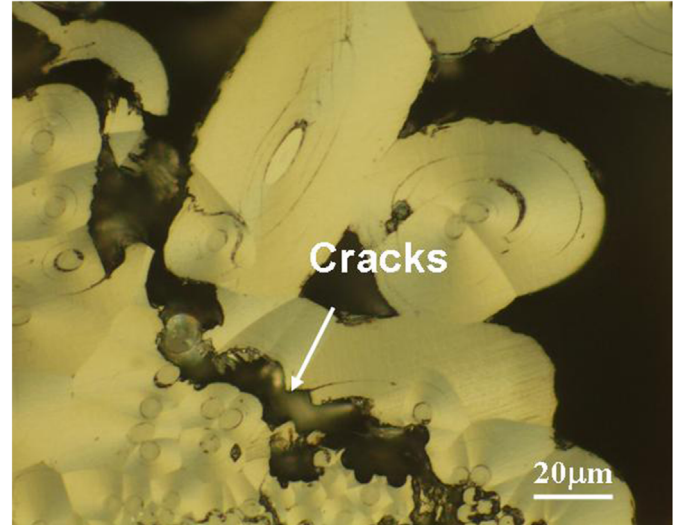


Fig. 4. Cracks in the C/C composites with addition of HfC.

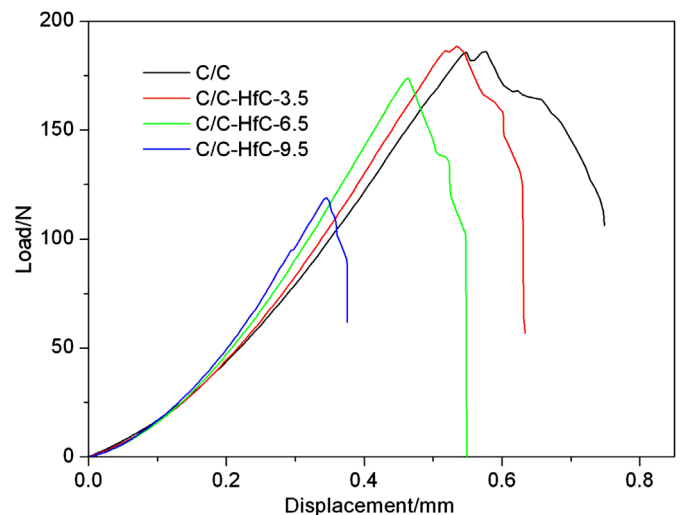


Fig. 5. Load–displacement curves of the C/C composites during flexural test.

Table 2
Mechanical properties of the C/C composites with different added contents of HfC.

Specimens	Content of HfC (wt%)	Specimen density (g/cm ³)	Compressive strength (MPa)	Compressive modulus (GPa)	Flexural strength (MPa)	Flexural modulus (GPa)
C/C	0.0	1.79	92	2.93	70	8.42
C/C–HfC-3.5	3.5	1.79	97	2.98	72	9.15
C/C–HfC-6.5	6.5	1.80	111	3.35	69	8.56
C/C–HfC-9.5	9.5	1.81	102	3.13	51	9.47

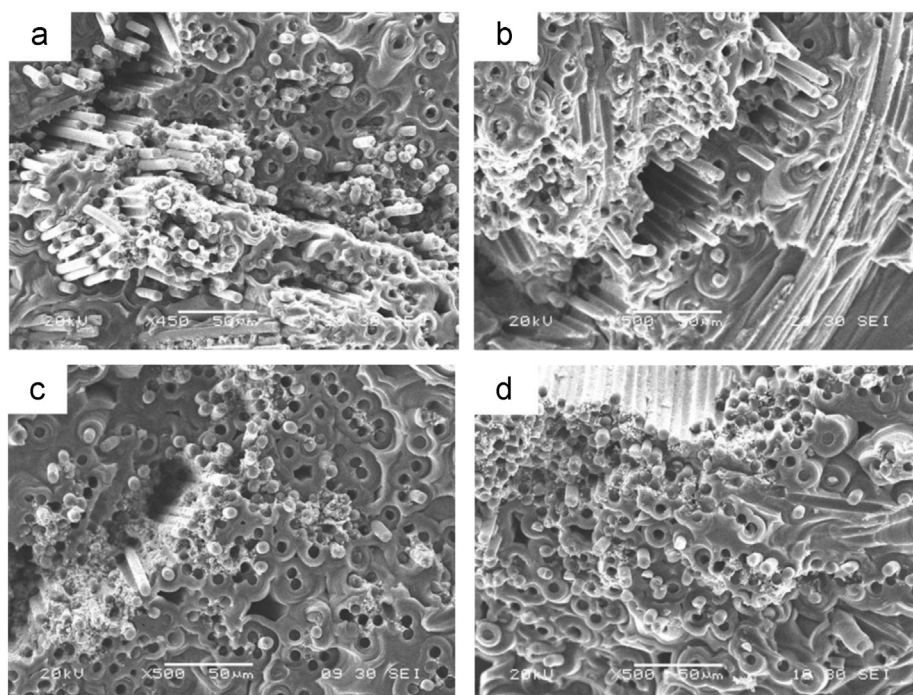


Fig. 6. Fracture morphology of the C/C composites with different added contents of HfC: (a) pure C/C, (b) 3.5 wt%, (c) 6.5 wt%, and (d) 9.5 wt%.

addition of HfC presents a smooth fracture surface and the fiber pull-out disappears gradually with the increase of HfC content (Fig. 6(b)–(d)). Moreover, HfC particle can be found on the surface of carbon fibers bundles. For the C/C composites with addition of HfC, chemical interactions can occur among fibers, matrix and HfO₂ in graphitization, which strengthen the bonding between fiber and matrix and increase the flexural modulus of composites. However, the chemical reactions can destroy the carbon fiber and then decrease the loading capability of carbon fibers, which cause the decrease of flexural strength of the composites. Furthermore, cracks in the composites decrease the loading capacity. Therefore, the C/C composites with addition of HfC present a brittle fracture with low flexural strength and high flexural modulus.

3.4. Thermophysical properties

3.4.1. Coefficient of thermal expansion

Fig. 7 shows CTE of the C/C composites with different added contents of HfC. CTE of the composites gradually increase with the increase of temperature both in *X–Y* and *Z* directions. CTE of the composites dramatically increase with the increase of HfC content both in *X–Y* and *Z* directions. CTE of HfC is $7.7 \times 10^{-6} \text{ K}^{-1}$ in the range of 25–612 °C [10], which is greater than that of the carbon fiber and matrix. CTE of the composites abide by the rule of mixtures, which is affected by the content of HfC. The composite with addition of 9.5 wt% HfC presents the highest CTE both in *X–Y* and *Z* directions.

3.4.2. Specific heat capacity

Fig. 8 shows specific heat capacity of the composites with different added contents of HfC. Specific heat capacity of the composites increases with the increase of temperature. Specific heat capacity of the composites with addition of HfC is higher than that of pure C/C composites at the same temperature. HfC presents high specific heat capacity (0.182 J/g K) at room temperature [10]. Specific heat capacity of the composites increases with the increase of HfC contents according to the rule of mixtures. However, specific heat capacity of the composites decrease when the HfC addition is greater than 6.5 wt%. Specific heat capacity of the C/C composites depends on the type of fibers and matrix, as well as microstructure such as voids, cracks, and defects [13]. Large amount of cracks existing in the composites with addition of 9.5 wt% HfC obstruct heat absorbed of the C/C composites, which causes the decrease of specific heat capacity of the composites.

3.4.3. Thermal conductivity

Fig. 9 shows thermal conductivity of the composites with different added contents of HfC. Thermal conductivity of the composites increases first and then declines with the increase of temperature. The composites with addition of 6.5 wt% HfC show the highest thermal conductivity as compared to other composites in both *X–Y* and *Z* directions.

Thermal conductivity is dominated by three factors including density, specific heat, and thermal diffusivity. Density of the composites with different HfC contents is

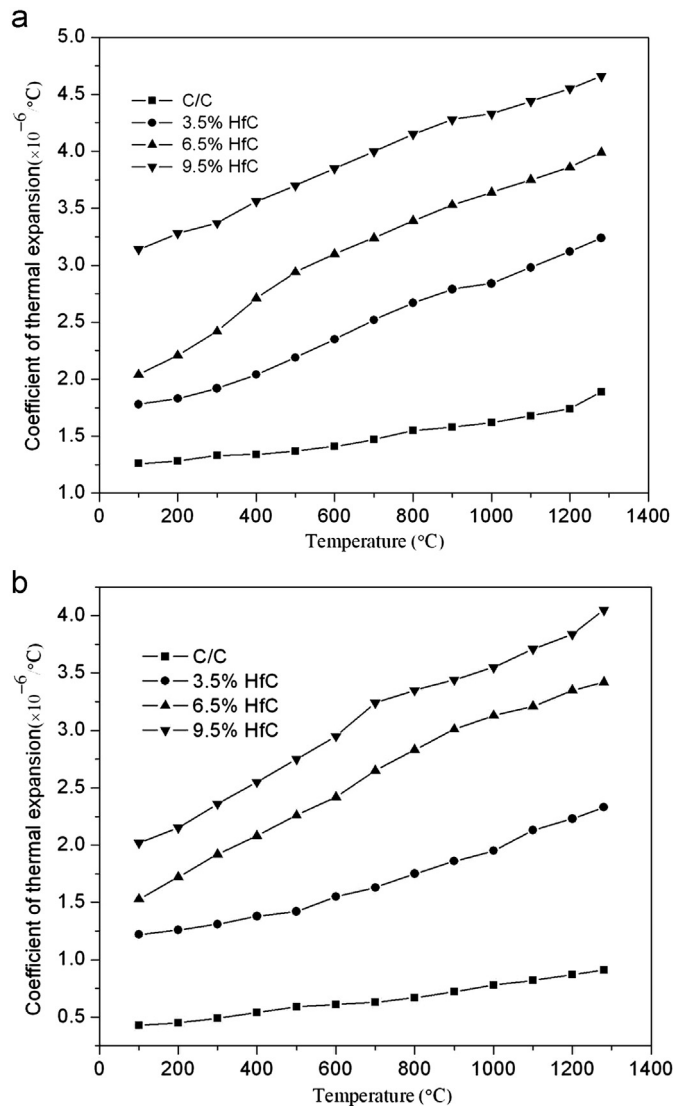


Fig. 7. CTE of the C/C composites with different added contents of HfC in (a) X–Y direction and (b) Z direction.

similar. Specific heat capacity of the C/C composites with addition of HfC is higher than that of pure C/C composites at the same temperature (Fig. 8). Thermal diffusivity acts make temperature uniform in materials. Thermal diffusivity of the composites decreases with the increase of temperature (Fig. 10). The composites with addition of 6.5 wt% HfC show the highest thermal diffusivity as compared to other composites at the same temperature. Therefore, thermal conductivity of the composites increases first and then declines with the increase of temperature according to Eq. (4). The composites with addition of 6.5 wt% HfC show the highest thermal conductivity.

Besides, thermal conductivity of the composites in the X–Y direction is higher than that in the Z direction. Carbon fiber is the channel of heat transmission in the C/C composites. The direction, dimension, and distribution of carbon fiber in the composites affect the thermal conductivity of materials. As for the integral needle

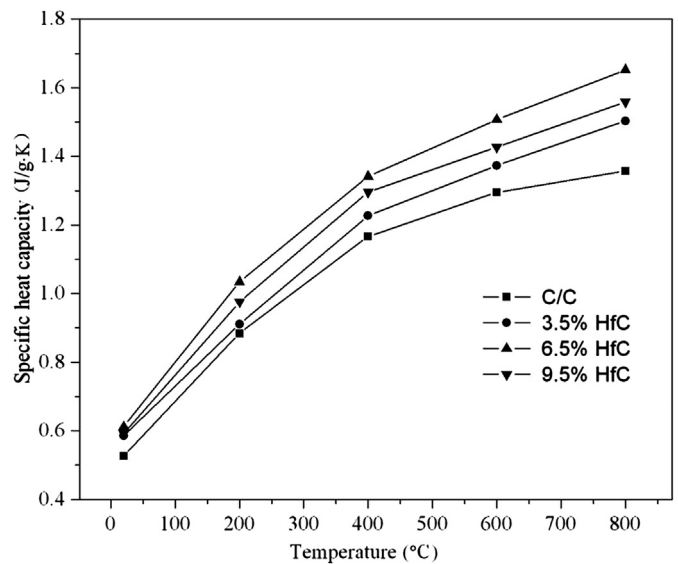


Fig. 8. Specific heat capacity of the C/C composites with different added contents of HfC.

punching carbon fiber felts, the number of carbon fibers distributed in the X–Y direction is greater than that of the needle-pricked carbon fibers in the Z direction. Therefore, the thermal conductivity of the composites in the X–Y direction is greater than that in the Z direction.

3.4.4. Heat conduction mechanism

Phonon interaction is responsible for the heat conduction in C/C composites. Phonon interaction in the C/C composites involves phonon–phonon interaction, phonon–defect interaction, and phonon–interface interaction [14]. Phonon interaction depends on the phonon mean free path, which is sensitive to temperature. The phonon vibration frequency is increased with the increase of temperature, which increases the collision possibility. So, the mean free path decreases rapidly, which leads to the decrease of thermal diffusivity. However, the specific heat capacity increases with the increase of temperature. Therefore, the thermal conductivity of composites first increases and then declines with the increase of temperature.

The thermal conductivity of HfC is 21 W/K m at room temperature, and reaches 27 W/K m at 800 $^\circ\text{C}$ with linear increase [9]. The thermal conductivity of HfC is lower than that of graphite. Adding HfC to improve the thermal conductivity of C/C composites is limited. Moreover, adding HfC into the C/C composites can increase the interface defects and change the carbon matrix into isotropic microstructure, which increases the phonon scattering and hence decreases the thermal conductivity.

However, formation of HfC accompanies generation of CO in graphitization, as shown:



The synthesised CO can be absorbed by the composites and store in the gaps and pores of the composites.

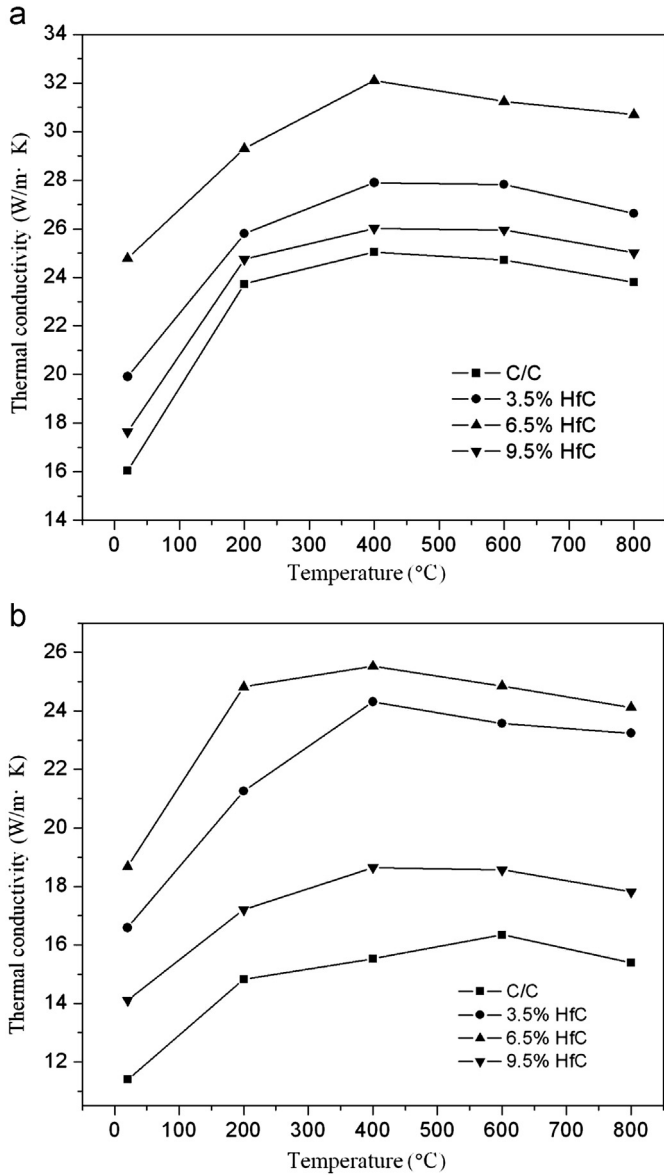


Fig. 9. Thermal conductivity of the C/C composites with different added contents of HfC in (a) X–Y direction and (b) Z direction.

The thermal diffusion of gas is related to the random thermal motion and collisions of molecules. CO, acting as a thermal diffusion medium, can improve the phonon–defect interaction in the C/C composites, which results in the increase of thermal conductivity of the composites.

Formation of CO increases with the increase of HfC content and the probability of molecular collision increases, which intensifies the phonon–defect interaction. When the content of HfC is less than 6.5 wt%, the increase of thermal conductivity is resulted from the thermal motion of CO in gaps and pores. Thermal conductivity of the composites decreases when HfC addition is greater than 6.5 wt%. It is resulted from the increase of cracks in the composites. Cracks increase the phonon scattering and hence decrease the thermal conductivity.

The generation of cracks can be attributed to two ways. On one hand, the thermal stress in composites can lead to

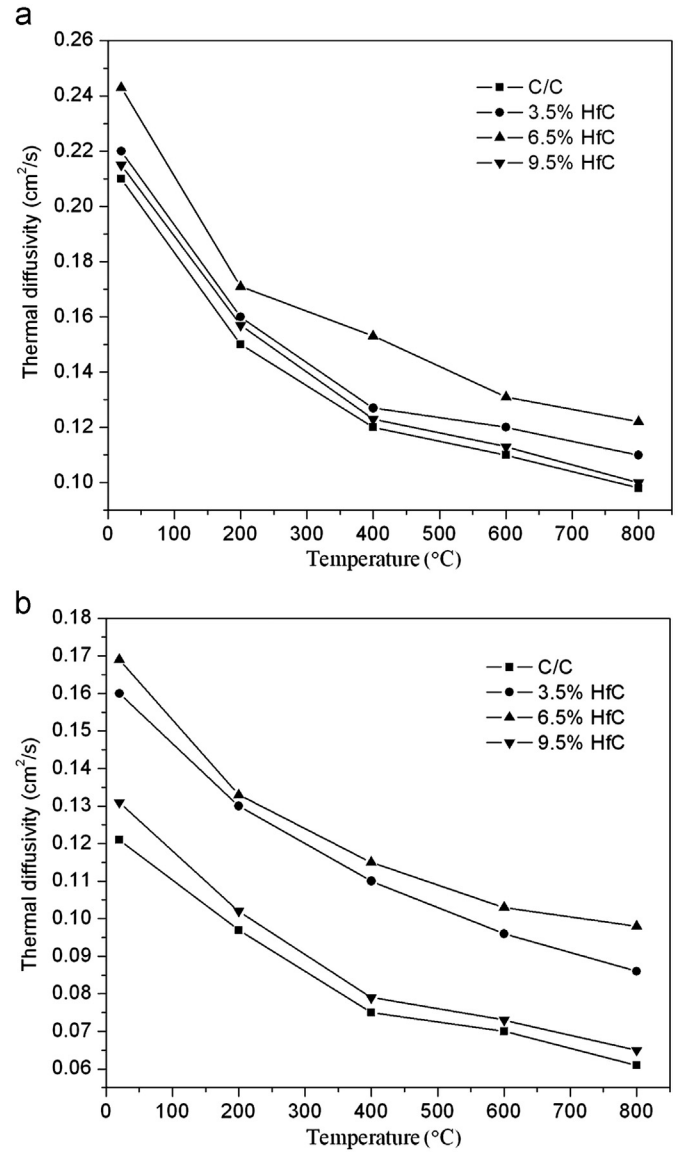


Fig. 10. Thermal diffusivity of the C/C composites with different added contents of HfC in (a) X–Y direction and (b) Z direction.

the generation of cracks, due to the mismatch of CTE between pyrolytic carbon matrix and HfC. On the other hand, cracks come from the gas pressure of generated CO. With the increase of HfC content, the thermal stress and gas pressure increase. Cracks are easy to generate when the stress exceeds the strength of composites. It is known that the thermal conductivity of composites is sensitive to cracks. The larger the cracks formed in the composites, the poorer the thermal conductivity of composites [14].

4. Conclusions

Mechanical properties, CTE and thermal conductivities of the C/C composites with addition of HfC were investigated. Compressive and flexural strength of the composites decrease dramatically when HfC content is greater than

6.5 wt%, which is attributed to the increase of cracks in the composites. The composites with addition of HfC present a brittle fracture. CTE of the composites increases with the increase of HfC content. The composites with addition of 6.5 wt% HfC show the highest thermal conductivity. The increase of thermal conductivity is attributed to the improved phonon–defect interaction produced by the thermal motion of CO in gaps and pores of the C/C composites. When the HfC addition is greater than 6.5 wt%, thermal conductivity of the composites decreases due to formation of a large number of cracks. Thermal conductivity of the composites in the X – Y direction is higher than that in the Z direction. The amount of carbon fibers in the X – Y direction is more than that in the Z direction, which can provide more channels for the heat transmission in the composites.

Acknowledgments

This research was supported by National Natural Science Foundation of China under Grant nos. 50832004 and 50972120, and the Program of Introducing Talents of Discipline to University under Grant no. B08040 and National “973” Project of the People’s Republic of China, under Grant no. 2011CB605806.

References

- [1] G. Savage, Carbon–carbon Composites, Chapman and Hall, London, 1993, pp. 331–57.
- [2] E. Fitzer, L.M. Manocha, Carbon Reinforcements and Carbon/carbon Composites, Springer, Berlin, 1998, pp. 250–319.
- [3] X.T. Shen, K.Z. Li, H.J. Li, H.Y. Du, W.F. Cao, F.T. Lan, Microstructure and ablation properties of zirconium carbide doped carbon/carbon composites, Carbon 48 (2010) 344–351.
- [4] Q.F. Tong, J.L. Shi, Y.Z. Song, Q.G. Guo, L. Liu, Resistance to ablation of pitch-derived ZrC/C composites, Carbon 42 (2004) 2495–2500.
- [5] S.P. Li, K.Z. Li, H.J. Li, Y.L. Li, Q.L. Yuan, Effect of HfC on the ablative and mechanical properties of C/C composites, Materials Science and Engineering A 517 (2009) 61–67.
- [6] Y.G. Wang, X.J. Zhu, L.T. Zhang, L.F. Cheng, Reaction kinetics and ablation properties of C/C–ZrC composites fabricated by reactive melt infiltration, Ceramics International 37 (2011) 1277–1283.
- [7] J. Yin, X. Xiong, H.B. Zhang, B.Y. Huang, Microstructure and ablation performances of dual-matrix carbon/carbon composites, Carbon 44 (2006) 1690–1694.
- [8] M. Mallik, A.J. Kailath, K.K. Ray, R. Mitra, Electrical and thermo-physical properties of ZrB₂ and HfB₂ based composites, Journal of the European Ceramic Society 32 (2012) 2455–2545.
- [9] M.M. Opeka, I.G. Talmy, E.J. Wuchina, J.A. Zaykoski, S.J. Causey, Mechanical, thermal, and oxidation properties of refractory hafnium and zirconium compounds, Journal of the European Ceramic Society 19 (1999) 2405–2414.
- [10] L.F. He, Y.W. Bao, J.Y. Wang, M.S. Li, Y.C. Zhou, Microstructure and mechanical and thermal properties of ternary carbides in Hf–Al–C system, Acta Materialia 57 (2009) 2765–2774.
- [11] S.E. Landwehr, G.E. Hilmas, W.G. Fahrenholtz, I.G. Talmy, H. Wang, Thermal properties and thermal shock resistance of liquid phase sintered ZrC–Mo cermets, Materials Chemistry and Physics 115 (2009) 690–695.
- [12] G.M. Song, Y.J. Wang, Y. Zhou, The mechanical and thermophysical properties of ZrC/W composites at elevated temperature, Materials Science and Engineering A 334 (2002) 223–232.
- [13] L.M. Manocha, A. Warrier, S. Manocha, D. Sathiyamoorthy, S. Banerjee, Thermophysical properties of densified pitch based carbon/carbon materials—I. Unidirectional composites, Carbon 44 (2006) 480–487.
- [14] R.Y. Luo, T. Liu, J.S. Li, H.B. Zhang, Z.J. Chen, G.L. Tian, Thermophysical properties of carbon/carbon composites and physical mechanism of thermal expansion and thermal conductivity, Carbon 42 (2004) 2887–2895.